# Design and Characterization of Arbitrary Filters with an Integrated Spiral $Si_3N_4/SiO_2$ Waveguide

**Yiwen Hu,[1,*] Shengjie Xie[1], Jiahao Zhan[1], Yang Zhang[1], Sylvain Veilleux,[2] and Mario Dagenais[1]**
[1]*Department of Electrical and Computer Engineering, University of Maryland, College Park, MD 20742, USA*
[2]*Department of Astronomy, University of Maryland, College Park, MD 20742, USA*
*yiwenhu@ece.umd.edu

**Abstract:** We report the optimization of reconstruction algorithm and experiment for an integrated arbitrary filter. A 43-notch filter near 1550 nm is implemented with an ultra-low-loss $Si_3N_4/SiO_2$ spiral waveguide. All notches have uniform depths/widths of about 20 dB/0.2 nm.

## 1. Introduction

Optical filters have many applications in telecommunications, optical signal processing, lasers, sensing and astrophotonics. A majority of work in these fields are done with fiber Bragg gratings (FBGs). With the strong push from the fiber optic communication industry in the last several decades, now people can make very long, complicated and accurate FBGs [1]. However, in recent years there is an ever-increasing demand for on-chip optical interconnection which can realize most possible functions in a tiny footprint. Within these objectives, high performance integrated arbitrary filters are an important aspect. For example, in astrophotonics, people need several hundred precise lines with precise depth and position to suppress the OH emission lines in the atmosphere, which up to now can only be achieved with complex waveguide Bragg gratings [1–3].

Among various algorithms for grating filter reconstruction, the layer peeling (LP) algorithm is one of the most popular because of its accuracy, robustness and speed [3,4]. However, there are some additional issues when applying it to design broad spectral range, narrow linewidth and high rejection filters, such as the errors related with the discretization of numerical modeling, lithography resolution and stability. In this work, we will address some of these issues for obtaining a better matched filter response.

## 2. Theoretical background and modeling

For grating filter design, a properly chosen direct scattering (DS) algorithm is as important as the inverse scattering (IS) algorithm itself. An effective DS can help us conveniently value the performance of different IS models. Here we use two DS methods to validate our layer peeling IS algorithm. The first one is the conventional piecewise coupled mode transfer matrix (CMT), which is the most intuitive validation model for the LP as a CMT's segment is the same as a LP's segment [4]. The other one is the ABCD matrix approach, in which we sample the sinusoidal-like grating in short enough rectangular segments, and calculate the transfer matrix between each segment by using the electromagnetic boundary conditions [5]. Specifically, in the LP and CMT validation, we use a layer size $\Delta z = 4$ μm; in the ABCD validation, we choose a segment size $\delta z = 100$ nm. ABCD validation is more time consuming, but it is a more flexible approach because it does not require any periodicity in the grating structure.

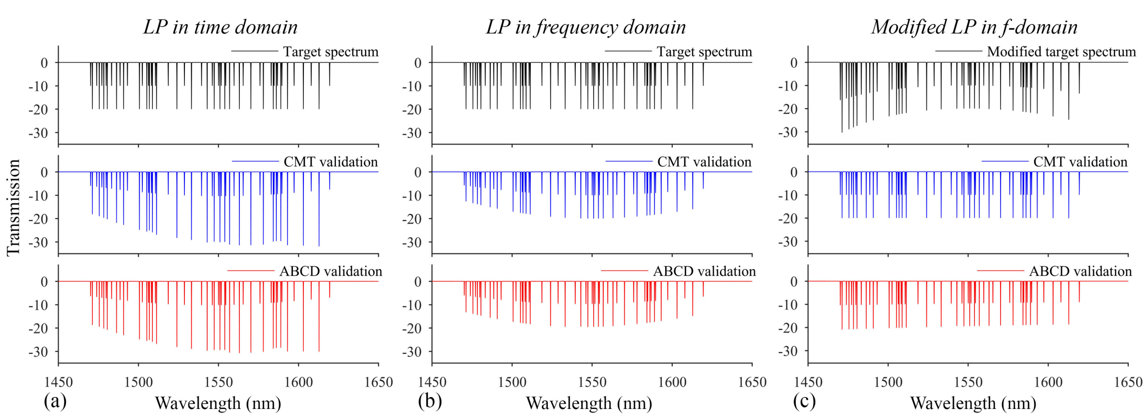


Fig. 1. Comparison of several different layer peeling (LP) algorithms for a 55-notch filter design with 10dB/20dB alternating notch depths. (a) LP in time domain. (b) LP in frequency domain. (c) LP in frequency domain with a sinc function modified target spectrum. It can be seen that only the modified LP can match the original target spectrum without any non-uniformity issue.

People have been using time domain and frequency domain LP to tackle inverse scattering problems, and time domain LP is generally preferred for speed purpose [4,6]. However, we find that the frequency domain LP gives more robust results, and it is very important if precise control over individual notch lineshape is a top priority. As an example, in Fig. 2(a, b) we use both time domain and frequency domain LP to reconstruct a 55-notch filter with alternating notch depths of 10 dB and 20 dB. For the time domain LP, the 10 dB dips are always well matched, but most 20 dB dips fail to match the target spectrum, indicated by both the CMT and the ABCD validations. This issue can be mitigated by introducing group delay terms, but it will increase the grating length, which is not desired for on-chip integration [7]. On the other hand, frequency domain LP gives stable results for both depths. As a result, frequency domain LP is the algorithm we selected for all following designs.

Another obvious issue is the non-uniform notch depths, which can be noticed in Fig. 1(b). For both CMT and ABCD validation spectra, the grating depth is only matched well with the target at the bandwidth center, and could become several dB shallower elsewhere, especially near the bandwidth boundaries. We found that this inconsistence is relevant with the non-zero layer size $\Delta z$ and exists for all numerical LP algorithms [4,7]. It can be mitigated by decreasing $\Delta z$, which however will increase the computing complexities and it cannot completely eliminate the issue. Interestingly, if we modify the original target spectrum with a $\text{sinc}(x)=\sin(x)/x$ function, this non-uniformity issue almost disappear for both validation plots, as shown in Fig. 1(c). A qualitative understanding in physics is that this error is caused by the discretization of the numerical modeling, and a sinc function is just the Fourier transform of a rectangular function related with a piecewise grating model.

### 3. Experimental results

For high rejection ratio filters with narrow linewidth, several centimeters or even longer gratings are usually required [3]. To reduce the footprint, we mapped the filter onto a spiral waveguide structure. As shown in Fig. 2(a), a 40 mm grating structure is overlaid on a layout consisting with two Archimedean spirals (in and out) and two connecting half circles. It is worth noting that this in-plane straight to curve mapping procedure is not a distance preserving transformation in mathematics, and will inevitably introduce geometric error. However, our experimental results in Fig. 2 and Fig. 3 imply that the error is negligible for our application.

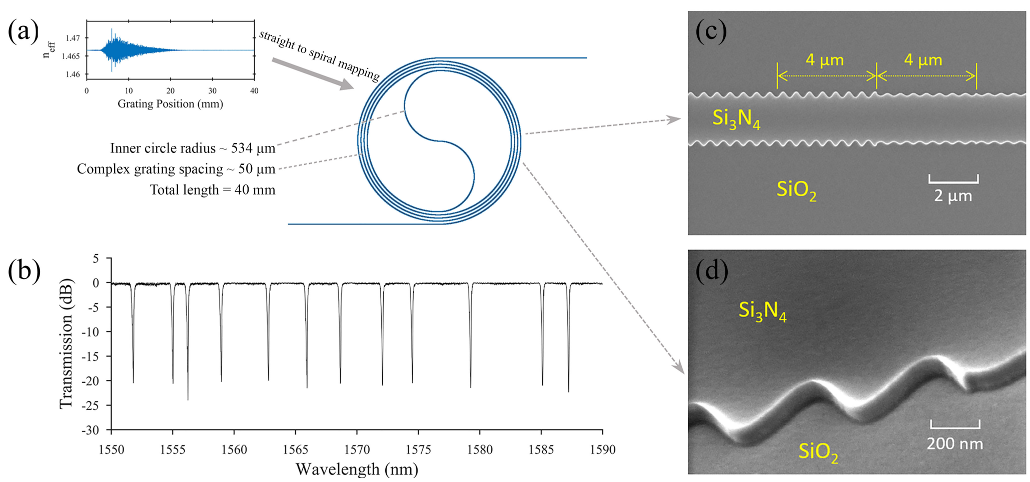


Fig. 2. (a) The illustration of spiral complex grating. The left-top inset shows the index profile of the 40 mm grating. (b) The normalized measure transmission from 1550 nm to 1590 nm shows 20 dB depth and 0.2 nm 3-dB width. (c,d) SEM of the fabricated spiral grating. Average width of $Si_3N_4$ core is 2 µm and etching height is 100 nm.

The spiral grating layout file is generated in FIMMPROP by assembling 10000 tiny gratings segment by segment. Each segment is 4 µm long and positioned according to the pre-calculated coordinates and angles. Since the critical bending radius of 2 µm × 100 nm $Si_3N_4/SiO_2$ waveguide is about 500 µm, the inner circle radius is set as 534 µm, which makes the whole device size about 1mm × 1mm. The footprint can be further reduced if we use high confinement waveguide design.

For the actual fabrication, the complete structure is patterned with an Elionix ELS-G100 electron-beam lithography (EBL) system, followed by inductively coupled plasma (ICP) etching and PECVD-TEOS $SiO_2$ cladding. SEM in Fig. 2(c,d) shows that the grating sidewall corrugation is well-defined and smooth, which is important for low-loss applications. Compared with our previous work [5], we are able to reduce the grating loss from 0.3 dB/cm to 0.1 - 0.15 dB/cm, when characterized with the same approach [5]. To the best of our knowledge, this is still the record loss level for integrated waveguide gratings. As for fiber-to-chip coupling, UHNA3 fiber is used for ultra-high coupling efficiency >90% per facet [8]. The measured transmission in Fig. 2 (b) shows that individual notches have ~ 20 dB rejection depth and ~ 0.2 nm 3 dB width.

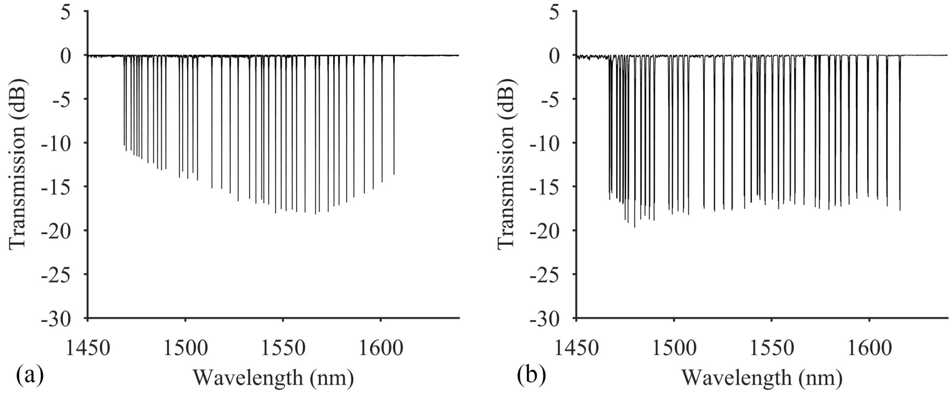


Fig. 3. The normalized measured spectrum with a design of (a) original target spectrum and (b) sinc function modified target spectrum.

To experimentally validate the approach which we have proposed to solve the non-uniform depth issue, we fabricated two spiral gratings of target notch depth 20 dB with and without the sinc function adjustment. The measured transmission in Fig. 3(a) shows that the non-uniformity issue indeed exists in the experiment, and the notch bottom contour is very similar with CMT and ABCD validation plots in Fig. 1(b). In comparison, Fig. 3(b) clearly exhibits a spectrum improvement after the sinc function adjustment is added. These two graphs also confirms that our CMT and ABCD validation models are very close with the actual experiments. Note that we have normalized these spectra such that the individual notch depth can be easily compared.

## 4. Summary

We have optimized the inverse and direct scattering algorithm for on-chip complex filter design and have proposed an efficient approach to solve the non-uniform depth issue when designing filters with a large spectral range and narrow linewidths. In the experiment, we successfully mapped a complex arbitrary filter, which contains 43 notches from 1450 nm to 1640 nm, to a 40 mm long low-loss spiral waveguide. With the demonstrated capability of precise control over individual notches within such a broad spectral range, on-chip arbitrary filters can become important components for many WDM applications.

## References

[1] J. Bland-Hawthorn, S. C. Ellis, S. G. Leon-Saval, R. Haynes, M. M. Roth, H. G. Löhmannsröben, A. J. Horton, J. G. Cuby, T. A. Birks, J. S. Lawrence, P. Gillingham, S. D. Ryder, and C. Trinh, "A complex multi-notch astronomical filter to suppress the bright infrared sky," Nat. Commun. **2**(1), 1–7 (2011).

[2] P. Rousselot, C. Lidman, J.-G. Cuby, G. Moreels, and G. Monnet, "Night-sky spectral atlas of OH emission lines in the near-infrared," Astron. Astrophys. **354**, 1134–1150 (2000).

[3] T. Zhu, Y. Hu, P. Gatkine, S. Veilleux, J. Bland-Hawthorn, and M. Dagenais, "Arbitrary on-chip optical filter using complex waveguide Bragg gratings," Appl. Phys. Lett. **108**(10), 101104 (2016).

[4] J. Skaar, L. Wang, and T. Erdogan, "On the synthesis of fiber Bragg gratings by layer peeling," IEEE J. Quantum Electron. **37**(2), 165–173 (2001).

[5] Y.-W. Hu, Y. Zhang, P. Gatkine, J. Bland-Hawthorn, S. Veilleux, and M. Dagenais, "Characterization of low loss waveguides using Bragg gratings," IEEE J. Sel. Top. Quantum Electron. **24**(4), 1–8 (2018).

[6] A. Buryak, J. Bland-Hawthorn, and V. Steblina, "Comparison of inverse scattering algorithms for designing ultrabroadband fibre Bragg gratings," Opt. Express **17**(3), 1995–2004 (2009).

[7] A. D. A. G. Badebo, E. L. G. T. Uritsyna, and J. A. R. Ohn, "Fabrication of precise aperiodic multichannel fibre Bragg grating filters for spectral line suppression in hydrogenated standard telecommunications fibre," Opt. Express **26**(2), 165–173 (2018).

[8] T. Zhu, Y. Hu, P. Gatkine, S. Veilleux, J. Bland-Hawthorn, and M. Dagenais, "Ultrabroadband high coupling efficiency fiber-to-waveguide coupler using Si3N4/SiO2 waveguides on Silicon," IEEE Photonics J. **8**(5), 1–12 (2016).